

# GaPt Supported Catalytically Active Liquid Metal Solution Catalysis for Propane Dehydrogenation—Support Influence and Coking Studies

Narayanan Raman, Moritz Wolf, Martina Heller, Nina Heene-Würl, Nicola Taccardi, Marco Haumann, Peter Felfer, and Peter Wasserscheid\*



Cite This: *ACS Catal.* 2021, 11, 13423–13433



Read Online

ACCESS |



Metrics & More



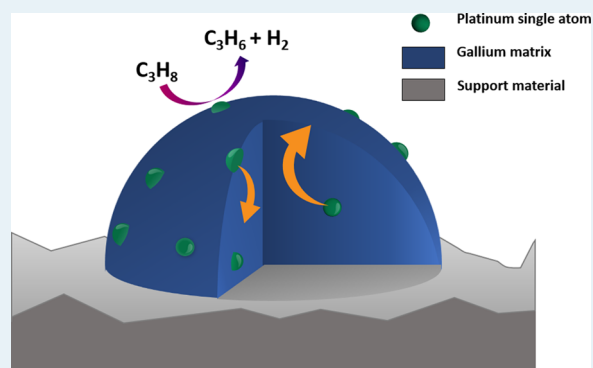
Article Recommendations



Supporting Information

**ABSTRACT:** Supported catalytically active liquid metal solutions (SCALMS) of Pt in Ga (2 at.-% Pt) were studied in the temperature range of 500 to 600 °C for propane dehydrogenation. A facile synthesis procedure using ultrasonication was implemented and compared to a previously reported organo-chemical route for gallium deposition. The procedure was applied to synthesize GaPt-SCALMS catalyst on silica (SiO<sub>2</sub>), alumina (Al<sub>2</sub>O<sub>3</sub>), and silicon carbide (SiC) to investigate the effect of the support material on the catalytic performance. The SiC-based SCALMS catalyst showed the highest activity, while SiO<sub>2</sub>-based SCALMS showed the highest stability and lowest cracking tendency at higher temperatures. The selectivity toward propene for the SiO<sub>2</sub>-based catalyst remained above 93% at 600 °C. The catalysts were analyzed for coke content after use by temperature-programmed oxidation (TPO) and Raman spectroscopy. While the SiC- and SiO<sub>2</sub>-supported SCALMS systems showed hardly any coke formation, the Al<sub>2</sub>O<sub>3</sub>-supported systems suffered from pronounced coking. SEM-EDX analyses of the catalysts before and after reaction indicated that no perceivable morphological changes occur during reaction. The SCALMS catalysts under investigation are compared with supported Pt and supported GaPt solid-phase catalyst, and possible deactivation pathways are discussed.

**KEYWORDS:** supported liquid catalysis, SCALMS, gallium, platinum, dehydrogenation, coking



## INTRODUCTION

The concept of supported catalytically active liquid metal solutions (SCALMS) was recently introduced for high-temperature catalysis.<sup>1</sup> Herein, a low melting and typically catalytically inactive metal (e.g., Ga) is doped with a small amount of a catalytically active metal (e.g., Pd, Rh, Pt),<sup>1–4</sup> and the resulting bimetallic alloy is deposited onto a porous support. The SCALMS material concept is shown schematically in Figure 1. In the SCALMS concept, the supported alloy is fully liquid at reaction temperatures. Note in this context that the melting point of these alloys is strongly dependent on the concentration and nature of the precious metal added. While pure gallium melts around 30 °C, addition of small amounts of another metal can increase the melting point of the resulting alloy to temperatures of 300 °C and beyond.<sup>5</sup>

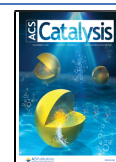
The precious metal is fully dissolved in the liquid Ga matrix under reaction conditions and is highly mobile, forming single atom sites at the liquid alloy-gas interface.<sup>6</sup> The concept provides a unique approach to achieve robust single-atom catalysis.<sup>7–9</sup> The single atom nature of the active site was first demonstrated by DFT calculation for GaPd systems and

supported for GaRh<sup>2</sup> and GaPt<sup>3</sup> systems using infrared reflection–absorption spectroscopy (IRAS).<sup>1,3</sup> In short, the outer layer of the liquid alloy droplets is typically depleted in atoms of the catalytically active metal.<sup>10</sup> In the presence of the reactants, however, the catalytically active metal atoms appear as single atoms at the gas–liquid metal interface to provide their catalytic reactivity to the system. Upon desorption of the formed products, the active metal atoms dive back into the bulk of the Ga-rich droplets resulting in a self-regenerating process of the catalytically active interface.<sup>11</sup>

SCALMS systems were successfully applied for butane and propane dehydrogenation, where the avoidance of rapid deactivation by coking is the primary challenge to realize effective catalytic materials.<sup>12–15</sup> In the state of the art, the

Received: April 28, 2021

Published: October 21, 2021



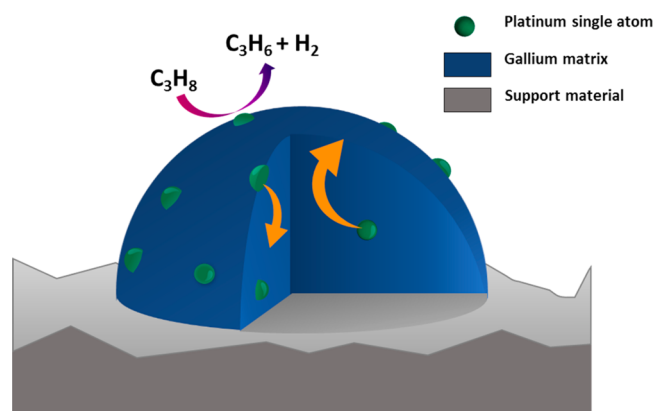


**Figure 1.** Schematic representation of GaPt-SCALMS catalysts for propane dehydrogenation. Single Pt atoms are shown in green within the blue Ga matrix. The dynamics of the system at high temperature is indicated by the trajectory of Pt moving from the bulk (orange arrows) to the surface and back.

catalysts are periodically regenerated by oxidation with air, which increases the complexity of the technical operation.<sup>16</sup> Alternatively, oxygen is cofed into the reactor to reduce coking, but this causes a loss of selectivity due to partial combustion of propane.<sup>17–19</sup>

The special nature of the active sites in SCALMS systems has been shown to reduce coke formation and to enhance catalyst lifetime under the harsh conditions of high-temperature dehydrogenation reactions.<sup>1,2</sup> The claim is that coke formation on the Ga-stabilized, single atom precious metal sites that form at the gas-alloy interface of SCALMS is suppressed because of the absence of vicinal catalyst sites required for the coke formation process. Note, however, that also the bare support surface is able to form coke from relevant precursor molecules, such as the products formed in alkane dehydrogenation.

In this contribution, we present a new, easy, and scalable approach to prepare gallium decorated supports and SCALMS systems. Our new methodology represents a very attractive alternative to the so far applied synthesis of SCALMS by impregnation with the very air sensitive compound  $(\text{Et}_3\text{N})\text{-GaH}_3$  as precursor for the Ga metal, obtained after thermal treatment, followed by galvanic displacement to introduce the catalytically active metal (in the following referred to as the chemical route). Our new approach builds on the fact that liquid metals, such as gallium, can be ultrasonicated to form colloidal dispersions in appropriate solvents.<sup>20–23</sup> The nano- and microdroplets obtained in this way can then be easily transferred to any support. Therefore, in this study, this method is applied to produce Ga-decorated support materials. The introduction of the catalytically active metal is achieved subsequently by galvanic displacement (Figure 2).<sup>24</sup> We compare the catalytic performance of GaPt-SCALMS systems prepared by the organo-chemical route with materials obtained from the newly developed ultrasonication method. Moreover, we use the newly developed preparation method for SCALMS materials to systematically study support effects in GaPt-SCALMS systems for propane dehydrogenation. In detail, we present the catalytic performance of SCALMS systems on silica ( $\text{SiO}_2$ ), alumina ( $\text{Al}_2\text{O}_3$ ), and silicon carbide ( $\text{SiC}$ ) supports.

## MATERIALS AND METHODS

All chemicals were used as received. SCALMS preparation was carried out using standard Schlenk techniques using Ar (99.999% purity, Linde Gas) as inert gas. Three different support materials, namely, alumina (Sigma-Aldrich; grade: Brockmann I, activated, standard; particle size: 0.05–0.15 mm; BET surface area:  $155 \text{ m}^2 \text{ g}^{-1}$ ; pH:  $7.0 \pm 0.5$ ), silica microspheres (Sigma-Aldrich; 0.06–0.17 mm), and silicon carbide (SICAT, France;  $\beta$ -SiC; pellet size: 3 mm), were applied in this study.

**Preparation of Catalysts by the Ultrasonication Method.** The supported Ga catalysts were prepared by

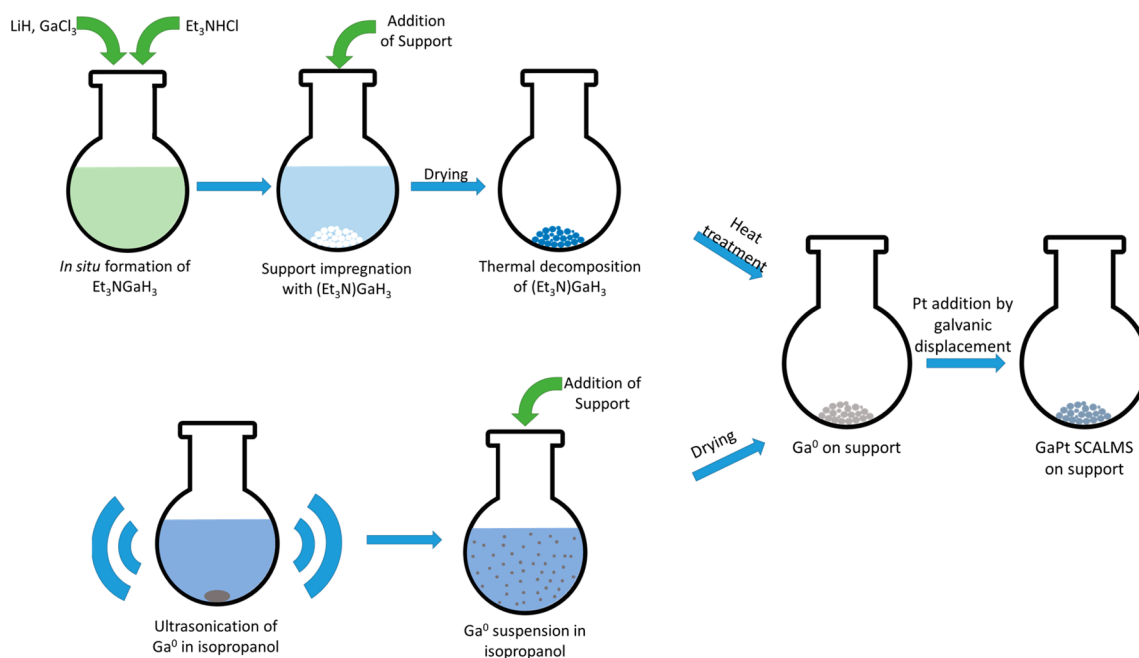


**Figure 2.** Schematic representation of the GaPt-SCALMS synthesis using the chemical route and the newly developed ultrasonication method.

physical deposition of metallic gallium on the different porous supports. A 6 mm Gallium nugget (5N, Alpha-Aesar) of approximately 0.8–0.9 g was dispersed in 100 mL isopropanol via ultrasonication (Branson 450 sonicator, 80% intensity for 10 min) at 40 °C and this created a fine emulsion of liquid Ga droplets. After sonication, the emulsion was added to the required amount of support material to achieve a 5% loading of Ga on support. Then, the solvent was slowly evaporated in a rotary evaporator at 50 °C. The obtained solid was calcined at 450 °C overnight.

The GaPt-SCALMS catalysts were prepared via galvanic displacement. A solution of hexachloroplatinic acid in water (2–3 mg Pt mL<sup>-1</sup>) was added to a suspension of 10 g of the respective Ga-decorated support in 50 mL of isopropanol targeting a desired Ga to Pt ratio of 45 (vide infra). The solvent was evaporated at 50 °C in a rotary evaporator. The resulting SCALMS was calcined at 450 °C overnight.

Additionally and for comparison, a GaPt SCALMS catalyst was also prepared on Al<sub>2</sub>O<sub>3</sub> using the chemical route as described by Bauer et al.<sup>3</sup> These platinum-decorated materials were also prepared by impregnation of the relevant support material with a hexachloroplatinic acid solution with subsequent drying at 50 °C and calcination at 450 °C overnight.

**Metal Content Analysis.** The Ga and Pt loadings of the prepared catalysts were determined by inductively coupled plasma atomic emission spectroscopy (ICP-AES) using a Ciroc CCD (Spectro Analytical Instruments GmbH). The solid samples were treated with a mixture of concentrated HCl:HNO<sub>3</sub>:HF using microwave heating up to 220 °C for 40 min to dissolve all metal from the catalyst for the analysis (the mixture was prepared based on volumetric ratios; **CAUTION:** HF is extremely harmful, and relevant safety precautions must be taken). The instrument was calibrated for Pt (214.423 nm) and Ga (417.206 nm) with standard solutions of the elements prior to the analysis.

**N<sub>2</sub>-Sorption Measurements to Determine Surface Area and Pore Size.** The surface area and average pore size of the supports were determined by isothermal low-temperature N<sub>2</sub>-sorption analysis at 77 K using a QUADROSORB SI Surface Area and Pore Size analyzer from Quantachrome Instruments. The multipoint-BET (Brunauer–Emmett–Teller) model was used to determine the specific surface area and the BJH method was used to determine the average pore size. All supports were pretreated at 250 °C for 12 h under high vacuum prior to the measurements.

**Temperature-Programmed Desorption (TPD) with CO<sub>2</sub> and NH<sub>3</sub>.** CO<sub>2</sub>- and NH<sub>3</sub>-TPD were performed using a Thermo Scientific TPDR0 1100 instrument equipped with a TCD sensor. Approximately 300 mg of material was weighed and dried at 500 °C under helium flow. The sample was cooled to 40 °C and loaded with CO<sub>2</sub> (or NH<sub>3</sub>) for a duration of 60 min and subsequently purged with helium for 15 min. The TPD data were obtained in a temperature range of 40 to 650 °C with a heating rate of 10 °C min<sup>-1</sup>.

**Scanning Electron Microscopy with Energy-Dispersive X-ray Spectroscopy (SEM-EDX).** The SEM-EDX measurements were performed on a ZEISS Cross Beam 540 Gemini II scanning electron microscope equipped with an EDX detector from Oxford Instruments Group. Silver paste (Acheson Silver DAG 1415) was used to enhance the electrical conductivity. Additionally, the samples were PVD carbon coated prior to the investigations. SEM images were obtained

at 3 kV and 2 nA. For BSD (Backscatter electron detector) images a voltage of 20 kV and a current of 2 nA was used. EDX analysis was performed at 20 kV and 1.1 nA. The EDX results show the Kα1 map for Ga and Mα1 map for Pt.

**Propane Dehydrogenation (PDH) in a Fixed Bed Tubular Reactor.** The as-prepared catalysts were tested for their activity in the propane dehydrogenation reaction. A continuous flow laboratory setup was used for these tests (see Figure S1, Supporting Information). The catalyst (1.2 g) was placed into the fixed-bed reactor (quartz glass of length 650 mm and inner diameter of 10 mm) that was positioned inside an electrically heated tubular split furnace (Carbolite). The reactor was heated to the set point of 500, 550, or 600 °C using a heating ramp of 10 °C min<sup>-1</sup>. After a stabilization time of 15 min, the reaction was started by supplying 8.9 mL<sub>N</sub> min<sup>-1</sup> propane (99.95% purity, Linde Gas) as feed gas diluted in 89 mL<sub>N</sub> min<sup>-1</sup> helium (99.996% purity, Linde Gas). The gas hourly space velocity (GHSV) was set to 4900 mL<sub>gas</sub> g<sub>Cat·bed</sub><sup>-1</sup> h<sup>-1</sup> resulting in a residence time (τ) of 0.7 s at standard conditions.

**Online Analysis of Reaction Products.** The product stream was analyzed by online gas chromatography (GC) using a Bruker 456 GC equipped with a GC-Gaspro column (30 m × 0.320 mm) and a flame ionization detector (FID). Mole fractions of compound *i* (*x<sub>i</sub>*) were calculated from peak areas and calibration factors, which were determined for every substance. The conversion of propane (*X<sub>propane</sub>*), the productivity, and the selectivity to propene (*S<sub>propene</sub>*) were calculated as follows:

$$X_{\text{propane}} = \frac{x_{\text{propane},0} - x_{\text{propane}}}{x_{\text{propane},0}} \cdot 100\% \quad (1)$$

$$S_{\text{propene}} = \frac{x_{\text{propene}}}{x_{\text{propane},0} - x_{\text{propane}}} \cdot 100\% \quad (2)$$

$$\text{productivity} = \frac{\dot{n}_{\text{propane},0} \cdot (X_{\text{propane}}/100) \cdot (S_{\text{propene}}/100) \cdot \text{MW}_{\text{propene}}}{m_{\text{Pt}}} \quad (3)$$

where *x<sub>i</sub>* is the mole fraction and *x<sub>i,0</sub>* is the initial mole fraction of compound *i* as calculated based on online-GC analysis, *n<sub>propane,0</sub>* is the total mole flow rate of propane in the feed, and MW<sub>propene</sub> is the molar weight of propene.

**Postrun, High-Resolution Thermogravimetric Analysis Coupled with Mass Spectrometry (HRTGA-MS).** Carbon deposits in the spent catalysts after PDH were characterized by means of high-resolution thermogravimetric analysis coupled with mass spectrometry (HRTGA-MS) using a XEMIS sorption analyzer (Hiden Isochema).<sup>25</sup> A total of ~200 mg of the sample was placed in a cylindrical stainless steel mesh sample holder, heated to 120 °C (5 °C min<sup>-1</sup>) under an inert He atmosphere for 6 h. Together with a subsequent heating to 500 °C (5 °C min<sup>-1</sup>) for 12 h, this procedure can be expected to remove adsorbed H<sub>2</sub>O from the sample under investigation. After the sample was cooled to 100 °C under a continuous He flow, 21% O<sub>2</sub>/He was introduced for 1 h at 100 °C. Subsequently, the temperature was increased with a heating rate of 1 °C min<sup>-1</sup> up to the maximum temperature of 500 °C for 12 h. The overall flow rate was 100 mL<sub>N</sub> min<sup>-1</sup> throughout TPO. A mass spectrometer (MS; Hiden Analytical) continuously analyzed the off-gas. The baselines of the MS signals were deducted in order to fit the

**Table 1. Characteristic Data for the Support Materials and the Catalyst Applied in This Study<sup>a</sup>**

system	concentration of basic sites (support/catalyst) $\mu\text{mol g}^{-1}$	concentration of acidic sites (support/catalyst) $\mu\text{mol g}^{-1}$	$S_{\text{BET}}$ $\text{m}^2 \text{g}^{-1}$	$V_{\text{pore}}$ $\text{mL g}^{-1}$	$d_{\text{pore}}$ $\text{nm}$	$D_{\text{particle}}$ $\mu\text{m}$
$\text{Al}_2\text{O}_3$	94/103	480/507	136	0.28	5	50–150
$\text{SiO}_2$	6/6	21/80	287	0.98	9	75–200
SiC	5/7	7/75	23	0.20	38	500–630

<sup>a</sup> $S_{\text{BET}}$  = specific surface area determined by BET method;  $V_{\text{pore}}$  = specific pore volume determined by BJH method;  $d_{\text{pore}}$  = average pore diameter determined by BJH method;  $D_{\text{particle}}$  = particle size range determined by sieving.

peaks in MATLAB<sup>26</sup> with the peakfit.m<sup>27</sup> algorithm of the file exchange database. Lastly, the quantification of carbon deposits in the spent SCALMS was linked with the activity during PDH by calculating the selectivity toward coke ( $S_{\text{coke}}$ ) according to eq 4.

$$S_{\text{coke}} = \frac{x_{\text{coke}} \cdot m_{\text{bed}}}{M_{\text{C}}} \cdot 100\% \quad (4)$$

$$\int 3 \cdot F_{\text{C}_3\text{H}_8}(t) \cdot X_{\text{C}_3\text{H}_8}(t) dt$$

where  $x_{\text{coke}}$  is the fraction of coke as identified during HRTGAMS,  $m_{\text{bed}}$  is the bed loading during PDH of 1.2 g,  $M_{\text{C}}$  and  $M_{\text{C}_3\text{H}_8}$  are the molecular weights of carbon and propane, respectively,  $F_{\text{C}_3\text{H}_8}$  is the molar flow of propane in the feed, and  $X_{\text{C}_3\text{H}_8}$  is the conversion of propane.

**Postrun Raman Spectroscopy.** Qualitative analysis of carbon deposits in spent SCALMS was also conducted via Raman spectroscopy using an AvaRaman-532HERO-EVO (Avantes) system with an AvaRaman-PRB-532 (Avantes) probe. The Raman setup consists of a 532 nm (green) solid-state laser (Cobolt) and an AvaSpec-HERO (Avantes) spectrometer with a grating set of 1200 lines  $\text{mm}^{-1}$  (HSC1200-0.75). The spectrometer was equipped with a 50  $\mu\text{m}$  slit, and the detected wavelength range was 534–696 nm. The Raman spectra were collected in 20 repetitions at 15 mW laser power with an exposure time of 5 s.

## RESULTS AND DISCUSSION

**Catalyst Characterization.** Three supports, namely, alumina ( $\text{Al}_2\text{O}_3$ ), silica ( $\text{SiO}_2$ ), and silicon carbide (SiC), were used to prepare catalysts for propane dehydrogenation. The textural characteristics of the used support materials are shown in Table 1. All supports were characterized by  $\text{N}_2$ -sorption (see Figure S2, Supporting Information).  $\text{SiO}_2$  and  $\text{Al}_2\text{O}_3$  were used as provided by the supplier. SiC was purchased as 3 mm-pellets and ground to a smaller size. The fraction of 500–630  $\mu\text{m}$  size was selected as the suitable particle size. The applied  $\text{SiO}_2$  and  $\text{Al}_2\text{O}_3$  supports had an average pore size of less than 10 nm. SiC had much larger pores in the range of 30–50 nm. It must be noted here that although  $\text{SiO}_2$  and  $\text{Al}_2\text{O}_3$  provide high surface area, the gallium is most likely deposited to a large extent on the external surface as most of the liquid metal droplets generated by ultrasonication typically exceed the average pore diameters.<sup>22</sup> Our  $\text{CO}_2$ -TPD of  $\text{Al}_2\text{O}_3$  showed that the basic site concentration on  $\text{Al}_2\text{O}_3$  was 94  $\mu\text{mol g}^{-1}$ , which is significantly higher than that for the applied  $\text{SiO}_2$  and SiC (6 and 5  $\mu\text{mol g}^{-1}$ ).  $\text{CO}_2$ -TPD of the synthesized catalyst indicates that the deposition of Ga and Pt only marginally changes the basic site concentration. The acidic site concentration from  $\text{NH}_3$ -TPD on  $\text{Al}_2\text{O}_3$  was found to be 480  $\mu\text{mol g}^{-1}$  as opposed to 21 and 7  $\mu\text{mol g}^{-1}$  for  $\text{SiO}_2$  and SiC, respectively. After synthesis, all catalysts showed a significant increase in the acid site concentration. This

increase is largely due to indirect acid treatment that the material undergoes by the addition of hexachloroplatinic acid.

In addition to the SCALMS catalyst synthesized by ultrasonication, a SCALMS catalyst ( $\text{Ga}_{49}\text{Pt}$  on  $\text{Al}_2\text{O}_3$ ) was also synthesized by the chemical route as described in an earlier publication.<sup>3</sup> In order to discriminate the effect of each component in a SCALMS catalyst, Ga on a support and Pt on support materials were also synthesized on each of the three supports in addition to the SCALMS catalysts. The SCALMS catalysts were prepared with a targeted Ga/Pt ratio >40 to ensure a fully liquid system under the applied reaction conditions. According to the GaPt phase diagram known from the literature, such a composition becomes fully liquid at approximately 300 °C. The elemental composition of the different catalysts was determined by ICP-AES and is given in Table 2.

**Table 2. Composition of All Catalysts Investigated in This Study as Determined by ICP-AES Measurements**

system	Ga wt.-%	Pt wt.-%	Ga:Pt $\text{mol}_{\text{Ga}} \text{mol}_{\text{Pt}}^{-1}$
$\text{Ga}/\text{Al}_2\text{O}_3$	4.22	-	-
$\text{Pt}/\text{Al}_2\text{O}_3$	-	0.32	-
$\text{Ga}_{49}\text{Pt}/\text{Al}_2\text{O}_3$	2.11	0.12	49
$\text{Ga}/\text{SiO}_2$	4.50	-	-
$\text{Pt}/\text{SiO}_2$	-	0.20	-
$\text{Ga}_{48}\text{Pt}/\text{SiO}_2$	3.63	0.21	48
$\text{Ga}/\text{SiC}$	4.28	-	-
$\text{Pt}/\text{SiC}$	-	0.62	-
$\text{Ga}_{41}\text{Pt}/\text{SiC}$	2.21	0.15	41
$\text{Ga}_{49}\text{Pt-Chem}/\text{Al}_2\text{O}_3$	6.25	0.36	49

Scanning electron microscopy was applied to characterize the morphology of all catalysts prepared (Figure 3). The images reveal differences induced by the applied support materials. The  $\text{Al}_2\text{O}_3$  particles consist of clusters of crystallites of different orientation, resulting in a large number of corners and edges. The  $\text{SiO}_2$  particles are spherical on a macroscopic level. On the SiC, no clear facets or flat surface areas can be identified. Even at high magnifications,  $\text{SiO}_2$  shows a smooth surface, while the surface of  $\text{Al}_2\text{O}_3$  reveals unidirectional cracks of about 100 nm in width running across the flat surfaces. SiC has an uneven and rough surface. More interesting in the context of our study is the distribution of the metallic droplets over the external surface. The latter is inhomogeneous on all supports. While metallic droplets aggregate in the cracks of the  $\text{Al}_2\text{O}_3$  support, no such defects are present on  $\text{SiO}_2$  resulting in a more uniform distribution over the surface. The uneven surface of SiC also promotes aggregation. In general, aggregation to larger droplets hints toward weak interaction between the alloy droplets and the support surface. Note that all Ga droplets have been initially generated by the same

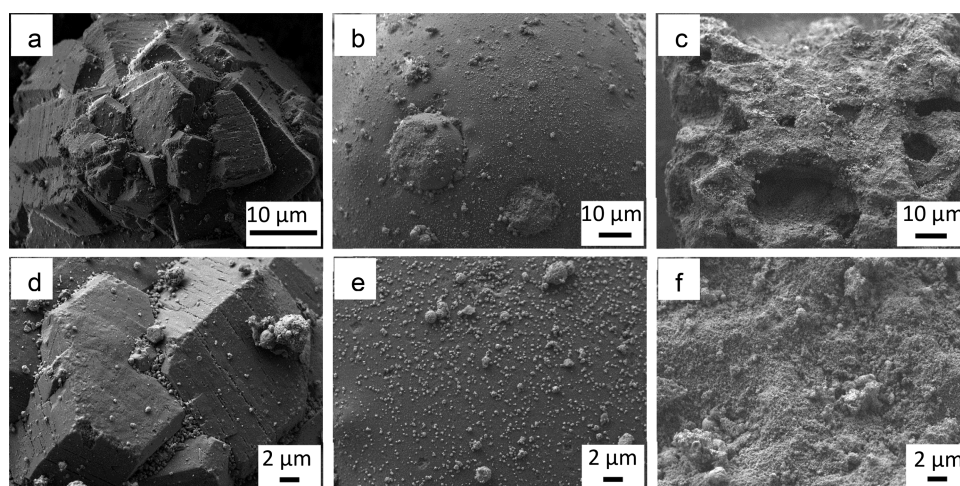


**Figure 3.** SEM images of as prepared GaPt-SCALMS catalyst supported on Al<sub>2</sub>O<sub>3</sub> (a,d), SiO<sub>2</sub> (b,e) and SiC (c,f) at low magnification (top row), higher magnification (bottom row).

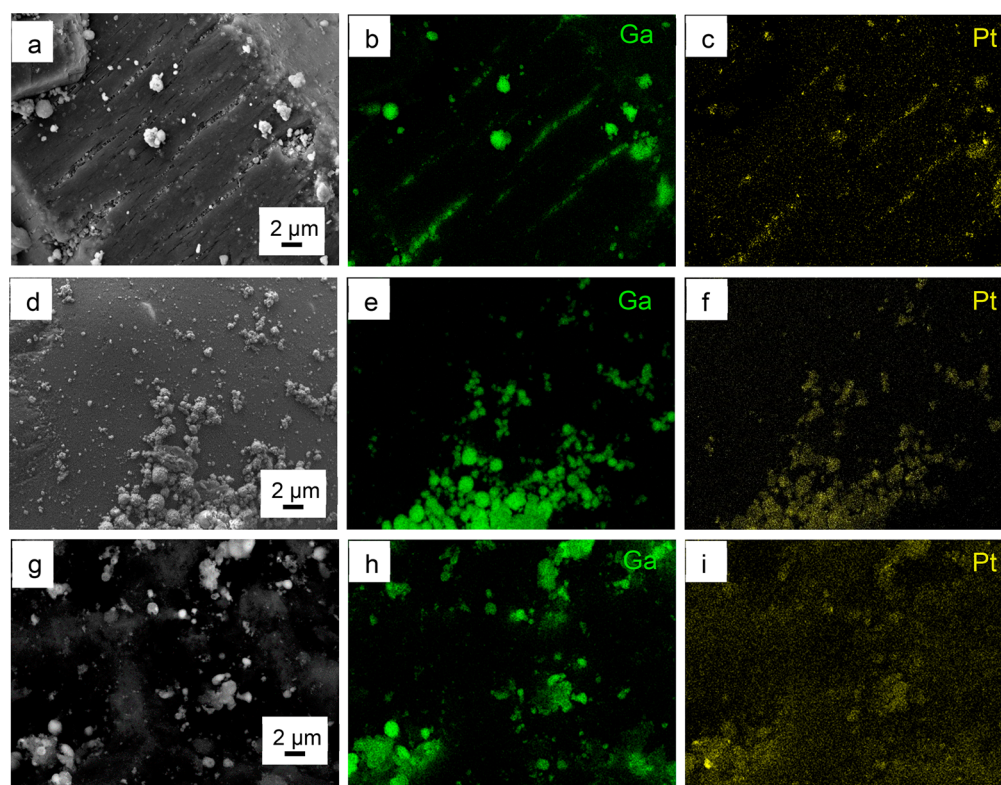


**Figure 4.** SEM-EDX images showing the distribution of gallium (Ga) and platinum (Pt) on Ga–Pt SCALMS catalyst supported on Al<sub>2</sub>O<sub>3</sub> (a–c), SiO<sub>2</sub> (d–f), SiC (g–i).

ultrasonication method in isopropanol under identical conditions prior to addition of the support material.

The distribution of gallium and platinum was further analyzed by SEM-EDX (Figure 4). As platinum is introduced to the materials by galvanic displacement, most of it is expected to be found at the gallium droplets. EDX mapping of the metals for the freshly prepared catalysts (Figure 4) as well as for the spent catalyst (see Figure S8, Supporting Information) shows indeed this collocation of Ga and Pt on the surface of the alloy droplets or crystallites for all materials.

#### Catalytic Results in Propane Dehydrogenation (PDH).

In order to determine potential effects of the new SCALMS

preparation route on the catalytic performance, we first compared the performance of Ga<sub>49</sub>Pt-SCALMS on Al<sub>2</sub>O<sub>3</sub> prepared by the traditional chemical route with the same composition prepared by our new ultrasonication method. Catalytic productivity and selectivity in propane dehydrogenation at 550 °C were evaluated (Figure 5, left). Interestingly, the catalyst prepared by ultrasonication showed an initial productivity close to 65 g<sub>propene</sub> g<sub>Pt</sub><sup>-1</sup> h<sup>-1</sup> compared with 50 g<sub>propene</sub> g<sub>Pt</sub><sup>-1</sup> h<sup>-1</sup> for the catalyst prepared by the chemical route. The propene selectivity was also slightly higher for the catalyst prepared by ultrasonication (Figure 5, right). In particular, the catalyst produced by the chemical route showed

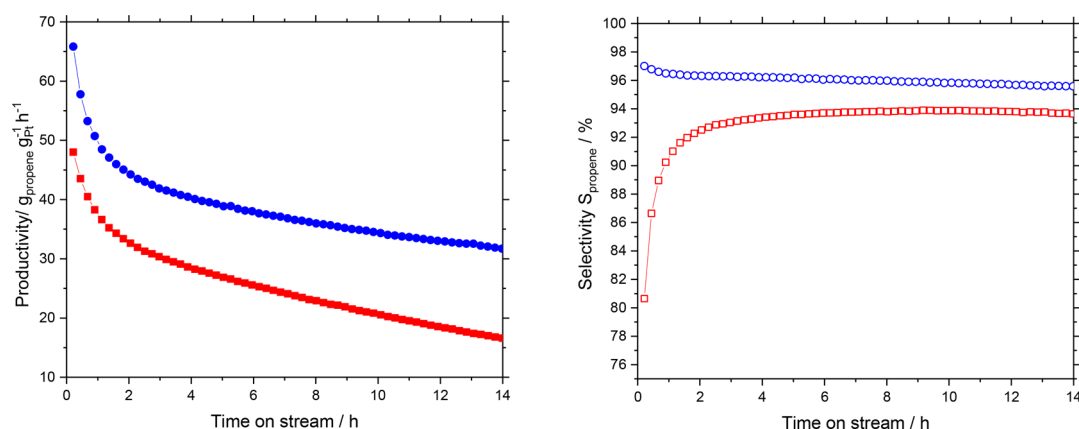


**Figure 5.** Productivity (filled symbols) and selectivity (open symbols) in propane dehydrogenation using different GaPt-SCALMS supported on  $\text{Al}_2\text{O}_3$  prepared by ultrasonication (blue symbols), and the chemical route (red symbols) at 550 °C and 1.2 bar. Reaction conditions: 1.2 g catalyst ( $\text{Ga}_{49}\text{Pt}/\text{Al}_2\text{O}_3$ : 2.11 wt-% Ga, 0.12 wt-% Pt;  $\text{Ga}_{49}\text{Pt-Chem}/\text{Al}_2\text{O}_3$ : 6.25 wt-% Ga, 0.36 wt-% Pt) He flow  $89 \text{ mL}_N \text{ min}^{-1}$ ,  $\text{C}_3\text{H}_8$  flow  $8.9 \text{ mL}_N \text{ min}^{-1}$ ,  $\text{GHSV } 4900 \text{ mL}_{\text{gas}} \text{ g}_{\text{Cat,bed}}^{-1} \text{ h}^{-1}$ .

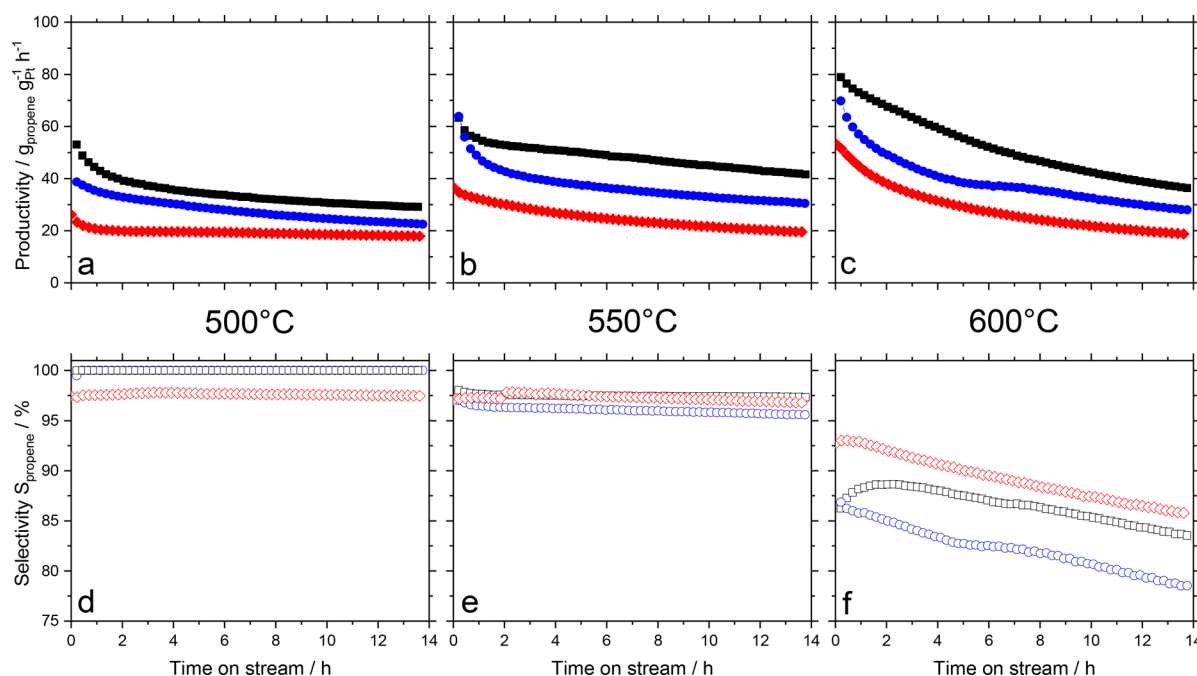


**Figure 6.** Productivity (filled symbols, a–c) and selectivity (open symbols, d–f) in propane dehydrogenation using different GaPt-SCALMS supported on  $\text{Al}_2\text{O}_3$  (blue symbols),  $\text{SiO}_2$  (red symbols), and  $\text{SiC}$  (black symbols) at 500 °C (a,d), 550 °C (b,e), and 600 °C (c,f) at 1.2 bar. Reaction conditions: 1.2 g catalyst ( $\text{Ga}_{49}\text{Pt}/\text{Al}_2\text{O}_3$ : 2.11 wt-% Ga, 0.12 wt-% Pt;  $\text{Ga}_{48}\text{Pt}/\text{SiO}_2$ : 3.63 wt-% Ga, 0.21 wt-% Pt;  $\text{Ga}_{41}\text{Pt}/\text{SiC}$ : 2.2 wt-% Ga, 0.15 wt-% Pt) He flow  $89 \text{ mL}_N \text{ min}^{-1}$ ,  $\text{C}_3\text{H}_8$  flow  $8.9 \text{ mL}_N \text{ min}^{-1}$ ,  $\text{GHSV } 4900 \text{ mL}_{\text{gas}} \text{ g}_{\text{Cat,bed}}^{-1} \text{ h}^{-1}$ .

a higher tendency toward cracking in the beginning. Overall, these results show that the preparation method based on Ga ultrasonication is a surprisingly attractive alternative to the somewhat tedious chemical preparation route to SCALMS materials. Note that the synthesis of the Ga precursor  $(\text{Et}_3\text{N})\text{GaH}_3$  needed for the chemical route requires protective dry/inert conditions and the use of a large excess of LiH, which affords very careful handling and produces significant amounts of noxious waste.<sup>28</sup> The production of SCALMS materials by ultrasonication, in contrast, is carried out in an alcoholic solvent without even the need for a protective atmosphere. This preparation route starts from elemental Ga and is characterized by almost perfect atom efficiency.

With the convenient and scalable SCALMS preparation via ultrasonication at hand, we proceeded with our further

investigations of support effects on the catalytic performance in propane dehydrogenation at temperatures of 500, 550, and 600 °C (Figure 6). Reference experiments with Ga/support and Pt/support catalysts under similar conditions were also conducted for comparison (see Supporting Information, Figures S12–17). At 500 °C (Figure 6a,d),  $\text{Ga}_{41}\text{Pt}/\text{SiC}$  showed the highest productivity of  $53 \text{ g}_{\text{propene}} \text{ g}_{\text{Pt}}^{-1} \text{ h}^{-1}$ , while the  $\text{Ga}_{49}\text{Pt}/\text{Al}_2\text{O}_3$  and  $\text{Ga}_{48}\text{Pt}/\text{SiO}_2$  SCALMS catalysts showed a productivity of 40 and  $25 \text{ g}_{\text{propene}} \text{ g}_{\text{Pt}}^{-1} \text{ h}^{-1}$ , respectively. At this temperature, all catalysts showed a propene selectivity exceeding 95%. The  $\text{SiO}_2$ -based catalyst, however, showed a very stable activity for 14 h after a slight initial deactivation. At 550 °C,  $\text{Al}_2\text{O}_3$  and  $\text{SiC}$ -based catalysts showed a very similar initial productivity of about  $65 \text{ g}_{\text{propene}} \text{ g}_{\text{Pt}}^{-1} \text{ h}^{-1}$ , while  $\text{SiO}_2$ -based catalyst had an initial productivity of  $40 \text{ g}_{\text{propene}} \text{ g}_{\text{Pt}}^{-1} \text{ h}^{-1}$ . In all

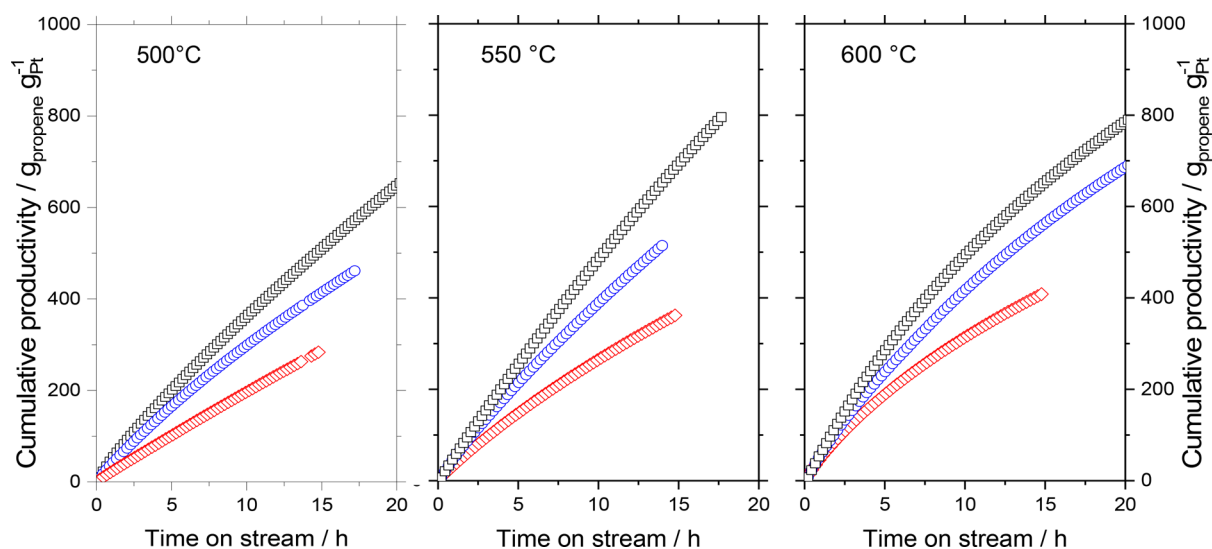


**Figure 7.** Cumulative productivity in propane dehydrogenation using different GaPt SCALMS supported on  $\text{Al}_2\text{O}_3$  (blue symbols),  $\text{SiO}_2$  (red symbols), and SiC (black symbols) at 500 °C (left), 550 °C (center), and 600 °C (right) and 1.2 bar. Reaction conditions: 1.2 g catalyst ( $\text{Ga}_{49}\text{Pt}/\text{Al}_2\text{O}_3$ : 2.11 wt-% Ga, 0.12 wt-% Pt;  $\text{Ga}_{48}\text{Pt}/\text{SiO}_2$ : 3.63 wt-% Ga, 0.21 wt-% Pt;  $\text{Ga}_{41}\text{Pt}/\text{SiC}$ : 2.2 wt-% Ga, 0.15 wt-% Pt) He flow  $89 \text{ mL}_N \text{ min}^{-1}$ ,  $\text{C}_3\text{H}_8$  flow  $8.9 \text{ mL}_N \text{ min}^{-1}$ ,  $\text{GHSV } 4900 \text{ mL}_{\text{gas}} \text{ g}_{\text{Cat}}^{-1} \text{ h}^{-1}$ .

cases, a certain deactivation over 14 h time on stream was observed, but  $\text{SiO}_2$  and SiC-based catalyst showed a more stable performance compared with the  $\text{Al}_2\text{O}_3$ -based catalyst. The activity levels remained in all cases above 50% of the initial activity. The propene selectivity was stable at values above 95% for all three catalysts under investigation (Figure 6b,e). At 600 °C, the  $\text{Al}_2\text{O}_3$  and SiC showed initial productivity in the range of 70 to 80  $\text{g}_{\text{propene}} \text{ g}_{\text{Pt}}^{-1} \text{ h}^{-1}$ , while  $\text{SiO}_2$  was the least active with an initial productivity just over 50  $\text{g}_{\text{propene}} \text{ g}_{\text{Pt}}^{-1} \text{ h}^{-1}$ . Loss in productivity of all three catalysts after 14 h time on stream was significantly higher than at 550 °C after the same time on stream. Remarkably, the propene selectivity was significantly lower than at 550 °C despite the very similar level of conversion, at least after 14 h time-on-stream. Moreover, the selectivity for SCALMS materials on all three supports showed a steady decline in contrast to the same materials at 550 °C (Figure 6c,f). It is an interesting observation that the formation of cracked products remained almost constant over time for all three materials tested at 600 °C. Thus, the declining selectivity trend is a consequence of a stable side product formation against a steadily reducing propene formation. This clearly indicates that most of the cracking takes place independent from the catalytic site responsible for the dehydrogenation reaction, probably directly at the support material. All catalysts showed some degree of deactivation at all temperatures. A closer analysis (see Supporting Information, Figures S2–4, for details) reveals two deactivation regimes at play. At 500 °C, the  $\text{SiO}_2$ -supported catalyst showed a fast initial loss of activity, followed by a rather stable performance, while both  $\text{Al}_2\text{O}_3$ - and SiC-based materials showed an exponential decay in activity (see Figures S3–S5 in Supporting Information). At higher temperature, all catalysts irrespective of their support showed a deactivation behavior that is best fitted by a second-order decay function (see Table S1 in Supporting Information). We assume coking on the bare support surface to be one major reason for the observed deactivation. This coke (see TPO studies below) fouls the catalyst surface, reduces thereby the accessibility of active sites and consequently lowers the activity.

Noteworthy, the specific surface area ( $S_{\text{BET}}$ ) of the support material does not seem to play a major role for the performance of the catalyst as SiC, the support with the lowest  $S_{\text{BET}}$ , is the most active catalyst. This is a consequence of the fact that Ga emulsification produces a majority of droplets that are bigger than the substrate pores<sup>20</sup> (see Supporting Information, Particle Size Distribution). Therefore, a significant part of the Ga droplets will remain on the external surface of the support, where they still contribute to the overall catalytic activity.

From the selectivity and conversion values, the cumulative productivity ( $\text{g}_{\text{propene}} \text{ g}_{\text{Pt}}^{-1}$ ) was calculated (see Figures 7 and S6–7 in the Supporting Information). Because of their high selectivity at 500 °C,  $\text{Ga}_{49}\text{Pt}/\text{Al}_2\text{O}_3$  and  $\text{Ga}_{41}\text{Pt}/\text{SiC}$  outperform the  $\text{SiO}_2$ -based catalyst after 15 h with cumulative productivities of 410 ( $\text{Al}_2\text{O}_3$ ) and 510 (SiC), whereas  $\text{Ga}_{48}\text{Pt}/\text{SiO}_2$  only yields 290  $\text{g}_{\text{propene}} \text{ g}_{\text{Pt}}^{-1}$ .  $\text{Ga}_{41}\text{Pt}/\text{SiC}$  as the most productive system was operated slightly longer and reached a cumulative productivity of 710  $\text{g}_{\text{propene}} \text{ g}_{\text{Pt}}^{-1}$  after 22 h, indicating good long-term performance. At 550 and 600 °C, higher initial productivities were obtained for all systems at still reasonable selectivities and stabilities. The stronger deactivation at 600 °C offsets the gain in initial activity at higher temperature. As a result, the cumulative productivity values at 600 °C are nearly the same compared with those obtained at 550 °C. At all temperatures under investigation, the SCALMS on SiC outperformed the two other support materials. The highest cumulative productivity was calculated for the SiC-supported SCALMS system with a value of 800  $\text{g}_{\text{propene}} \text{ g}_{\text{Pt}}^{-1}$  at 550 °C after only 18 h time-on-stream.

Table 3 summarizes the performance data for all catalysts under investigation for the three different temperatures.

Also the data in Table 3 indicate that among the tested materials and conditions the SiC-supported SCALMS catalyst at 550 °C is the best choice. SiC as support combines a low level of side product formation with good activity. At 500 °C, selectivity is excellent and stable, but reactivity is significantly lower. At 600 °C, a high initial activity is paired with

**Table 3. Propane Dehydrogenation Performance Data for the Different GaPt-SCALMS Catalysts Supported on Al<sub>2</sub>O<sub>3</sub>, SiO<sub>2</sub>, and SiC at Temperatures between 500 and 600 °C<sup>a</sup>**

T °C	catalyst	X <sub>0</sub> %	S <sub>0</sub> %	S <sub>14h</sub> %	CP <sub>14h</sub>
					g <sub>propene</sub> g <sub>Pt</sub> <sup>-1</sup>
500	Ga <sub>48</sub> Pt/SiO <sub>2</sub>	7.8	97.5	97.6	270
	Ga <sub>49</sub> Pt/Al <sub>2</sub> O <sub>3</sub>	6.4	99.5	99.9	390
	Ga <sub>41</sub> Pt/SiC	11.5	99.9	99.9	480
550	Ga <sub>48</sub> Pt/SiO <sub>2</sub>	11.4	97.1	96.7	350
	Ga <sub>49</sub> Pt/Al <sub>2</sub> O <sub>3</sub>	11.4	97.0	95.5	520
	Ga <sub>41</sub> Pt/SiC	14.1	98.0	97.3	650
600	Ga <sub>48</sub> Pt/SiO <sub>2</sub>	19.2	92.7	85.5	400
	Ga <sub>49</sub> Pt/Al <sub>2</sub> O <sub>3</sub>	14.4	86.9	78.4	540
	Ga <sub>41</sub> Pt/SiC	18.5	86.2	83.4	630

<sup>a</sup>T = reactor temperature; X<sub>0</sub> = initial conversion; S<sub>0</sub> = initial propene selectivity; S<sub>14h</sub> = propene selectivity after 14 h; CP<sub>14h</sub> = cumulative productivity after 14 h; CP data were smoothed to full digits.

significantly lower and falling selectivity combined with significant deactivation over time.

In the following, we aimed at elucidating the reasons for the different levels of deactivation observed for all SCALMS systems under investigation at the various process conditions. Two major reasons were considered: (i) coking of either active site or of the support limiting the access to the active site; (ii) coalescence of the liquid droplets in the SCALMS systems (especially for the part supported on the outer surface of the catalyst material). In order to gain the targeted insight into the relevant deactivation mechanisms at work, the spent catalyst was analyzed by TPO with HRTGA-MS for coke content determination and by SEM for morphological changes.

**Postrun, High-Resolution Thermogravimetric Analysis Coupled with Mass Spectrometry (HRTGA-MS).** The weight loss of a predried SCALMS sample in a TPO experiment in 21% O<sub>2</sub>/He at 500 °C for 12 h can be considered to correspond to the amount of coke present in the sample. This method was applied to determine the coke content and the CO<sub>2</sub> formation during TPO (as detected using the MS signal for a mass-to-charge ratio of 44) for all SCALMS samples after the respective catalytic runs. As seen from Figure 8 (see Supporting Information, Figure S9 for integral information on the CO<sub>2</sub> signal), coke formation increases with temperature and support-wise in the order SiO<sub>2</sub> < SiC < Al<sub>2</sub>O<sub>3</sub>. This result is not unexpected, as the acidic sites on alumina enhance coke formation. In-line with its excellent stability, hardly any coke was detected on GaPt/SiO<sub>2</sub> after PDH at 500 °C for 14 h (see Figure 6). Additionally, at 600 °C, only minor amounts of coke were detected (up to 0.12 wt-% after 14 h PDH operation) on this support despite the observed significant deactivation. This observation is well in-line with recent reports by some of us highlighting the high resistance of GaPt/SiO<sub>2</sub> SCALMS against coking, in contrast to Al<sub>2</sub>O<sub>3</sub>-supported SCALMS systems.<sup>29</sup>

The GaPt-SCALMS system on SiC showed after PDH at 600 °C a certain content of coke (net decrease of sample weight of 0.54 wt-% in TPO), while after PDH at 550 °C coke formation was minimal, well in-line with the catalytic results.

The SCALMS system on alumina shows after use in PDH at 600 °C in the subsequent TPO experiment a marked weight increase during the heating process (mainly in the temperature range of 250–350 °C, see Figure 8). Obviously, other processes affect the sample weight during TPO of spent SCALMS next to the oxidation of coke. Oxidation of gallium and/or the active metal are obvious options. Furthermore,

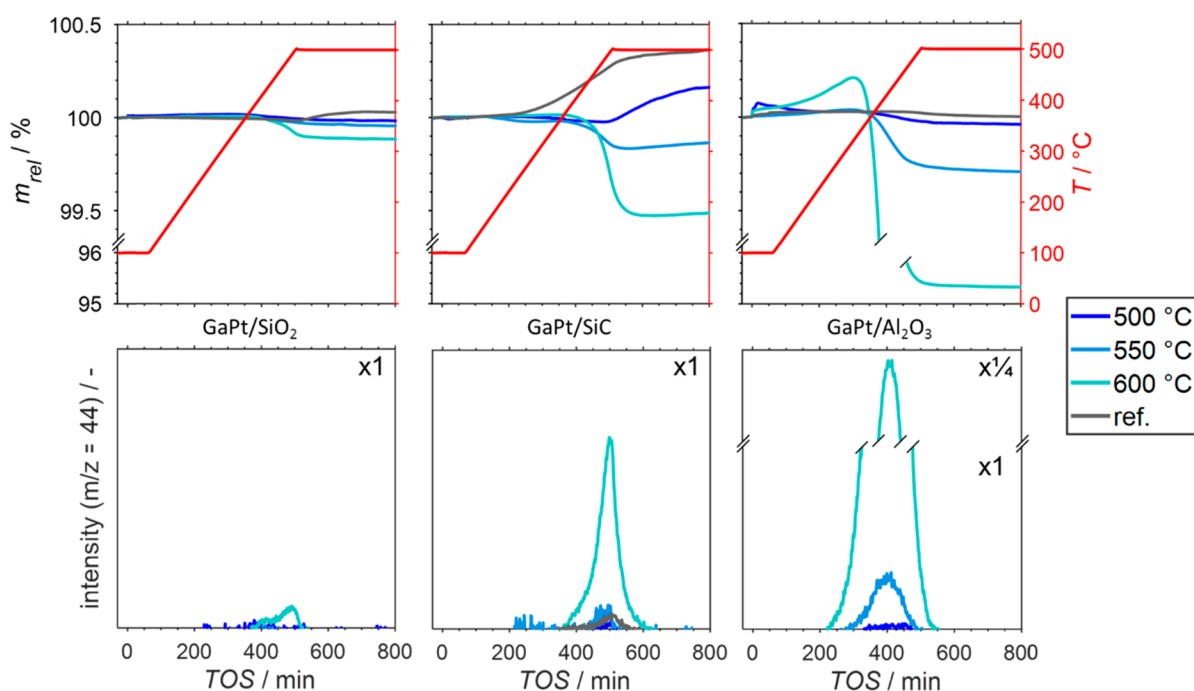


**Figure 8.** Sample weight relative to the weight prior to exposure to 21% O<sub>2</sub>/He at 100 °C (top) and formation of CO<sub>2</sub> (bottom) during temperature programmed oxidation (1 °C min<sup>-1</sup>) of spent Ga<sub>49</sub>Pt/Al<sub>2</sub>O<sub>3</sub> (left), Ga<sub>48</sub>Pt/SiO<sub>2</sub> (middle), and Ga<sub>41</sub>Pt/SiC (right). These SCALMS systems were investigated after propane dehydrogenation at 500 °C (dark blue), 550 °C (blue), and 600 °C (light blue) together with the bare support materials (gray) by HRTGA-MS. Conditions: 100 mL<sub>N</sub> min<sup>-1</sup> He (TOS < 0); 79 mL<sub>N</sub> min<sup>-1</sup> He and 21 mL<sub>N</sub> min<sup>-1</sup> O<sub>2</sub> (TOS > 0); WHSV 30 000 mL<sub>N</sub> g<sup>-1</sup> h<sup>-1</sup>.



formation of oxygen-containing functionalities on carbon<sup>15</sup> may also increase the sample weight during the temperature ramp to 500 °C. Such a formation of carbon functionalities upon first exposure to O<sub>2</sub> was previously identified during TPO of GaRh/Al<sub>2</sub>O<sub>3</sub>, GaPt/Al<sub>2</sub>O<sub>3</sub>, and GaPt/SiO<sub>2</sub> SCALMS.<sup>29,30</sup> Also, potential effects of the support material on the sample weight have to be taken into account. Herein, only the bare SiC support resulted in a significant weight increase during TPO (Figure 8), most likely due to an extended surface passivation of the support material by O<sub>2</sub> forming SiO<sub>2</sub> and CO<sub>2</sub>. The formation of the latter is also evidenced via MS. This strong effect of the support material results in an underestimation of the amount of coke formed when considering the net weight change only.

We previously hypothesized that coke formation over the Al<sub>2</sub>O<sub>3</sub> support material is enhanced during PDH at 550 °C compared with lower operation temperatures, that is, carbon deposition during PDH at elevated temperatures may be mostly caused by Al<sub>2</sub>O<sub>3</sub> itself.<sup>30</sup> Further, coking on Al<sub>2</sub>O<sub>3</sub> resulted in a highly reactive coke species, which could be oxidized at low temperatures as a result of highly reactive amorphous coke. The pronounced weight loss of 4.68 wt.-% of the GaPt/Al<sub>2</sub>O<sub>3</sub> SCALMS after PDH at 600 °C strongly supports this hypothesis, in particular when compared with the much smaller weight loss after PDH at 550 and 500 °C (0.29 and 0.04 wt.-%, respectively, Figure 8). The high reactivity of the coke formed on the SCALMS system in alumina after PDH at 600 °C is confirmed here by comparing the CO<sub>2</sub> formation in the TPO experiment as a function of temperature (Figure 9

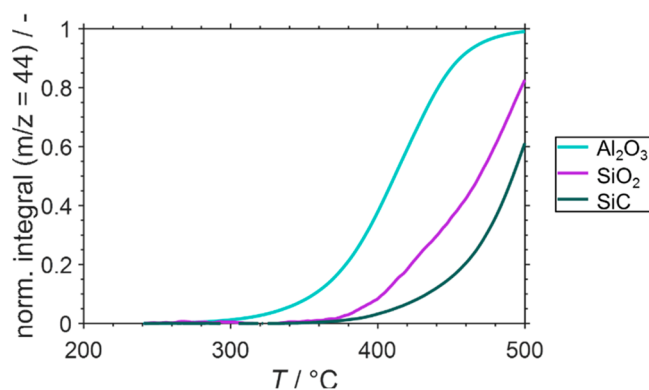


**Figure 9.** Normalized cumulative formation of CO<sub>2</sub> during temperature-programmed oxidation (1 °C min<sup>-1</sup>) of spent GaPt SCALMS using Al<sub>2</sub>O<sub>3</sub> (blue), SiO<sub>2</sub> (purple), and SiC (dark green) as support materials after propane dehydrogenation at 600 °C as monitored via high-resolution thermogravimetry coupled with mass spectrometry. Conditions: He flow 100 mL<sub>N</sub> min<sup>-1</sup> for TOS < 0; He flow 79 mL<sub>N</sub> min<sup>-1</sup> and O<sub>2</sub> flow 21 mL<sub>N</sub> min<sup>-1</sup> for TOS > 0; GHSV 30 000 mL<sub>N</sub> g<sup>-1</sup> h<sup>-1</sup>.

and Figure S9 in the Supporting Information). Much less reactive, graphitic coke is formed, in contrast, on the SiC-supported and, to a lower extent, on the SiO<sub>2</sub>-supported SCALMS (see Supporting Information, Figures S10–11 for Raman spectra of the spent SiC supported catalyst).

The results from TPO were linked with the catalytic performance data to calculate the integral selectivity of the prepared SCALMS systems toward coke using Equation 4. A clear correlation between the PDH reaction temperature and the selectivity for coke formation is identified on all supports (Table 4). The absolute levels of coke formation are, however,

**Table 4.** Integral Carbon-Based Selectivity toward Coke of the SCALMS Tested in This Study

system	temperature °C	S <sub>coke</sub> %
Ga <sub>49</sub> Pt/Al <sub>2</sub> O <sub>3</sub>	500	0.11
	550	0.49
	600	4.98
Ga <sub>48</sub> Pt/SiO <sub>2</sub>	500	<0.01
	550	0.11
	600	0.49
Ga <sub>41</sub> Pt/SiC	500	<0.01
	550	0.17
	600	0.46

quite different. For Al<sub>2</sub>O<sub>3</sub>-supported SCALMS, the selectivity for coke formation reached 4.98% at 600 °C, while coke formation is under identical temperature conditions about 1 order of magnitude lower on the SiC- and SiO<sub>2</sub>-supported systems.

#### Postrun SEM Analysis and Deactivation Mechanism.

After propane dehydrogenation, we selected the spent SiO<sub>2</sub>-supported SCALMS systems for further analytical studies to shed light on the deactivation mechanism during PDH. Because of its smooth surface, the SiO<sub>2</sub>-supported system would allow for easily recognizable agglomeration phenomena that might be responsible for the observed loss of activity. In our SEM investigation, however, it was found that the droplet size distribution of the catalytic materials did not undergo major changes and was very similar for all the catalysts after PDH at all the temperature tested when compared to the fresh SCALMS system (Figure 10a–c). Therefore, more subtle effects may cause the observed decline in performance. Recently, investigation using model GaPt SCALMS on highly oriented pyrolytic graphite (HOPG) evidenced that the liquid droplet can separate into Pt-rich and Ga-rich domains as the droplet migrates over the surface of the support.<sup>31</sup> It is possible that a similar phenomenon may also be at play on the surface of the supports tested in this study. This phase separation process may generate droplets of liquid alloy depleted in Pt and Pt-rich droplets that are presumably solid under the applied reaction conditions. The latter undergo irreversible deactivation via strong adhesion of carbonaceous species, while the liquid domain preserve their activity due the dynamicity of their surface

Further studies are currently ongoing in our laboratories to address these issues in more detail and to gain a better understanding of these highly dynamic catalytic systems.

## CONCLUSIONS

We have demonstrated in this work a new, facile, and scalable method to prepare GaPt SCALMS by ultrasonication. This new procedure represents a very convenient alternative to the previously reported chemical route employing an air sensitive gallane complex. The GaPt SCALMS materials synthesized via this new route enabled nearly identical catalytic activity in propane dehydrogenation at benchmark conditions compared to those prepared by the chemical route despite the fact that a large part of the alloy droplets was deposited on the external surface of the applied catalyst supports. Using this ultrasonication method, GaPt SCALMS catalyst were synthesized on three different supports (alumina, silica, SiC) and tested for propane dehydrogenation in the temperature range of 500–

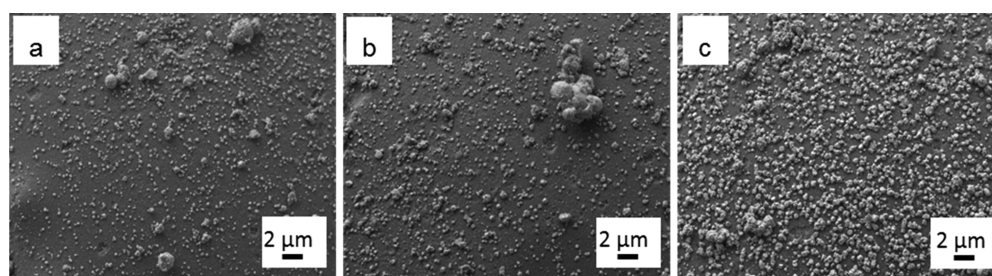


**Figure 10.** SEM images of GaPt catalyst supported on SiO<sub>2</sub> (a) as prepared, (b) after PDH at 500 °C, and (c) after PDH at 600 °C.

600 °C. HRTGA-MS analysis of all spent catalysts confirmed that the largest part of the observed coke originates from the support. Among the prepared SCALMS materials systems, the SiC-supported materials showed the highest Pt-based productivity followed by Al<sub>2</sub>O<sub>3</sub> and SiO<sub>2</sub>. The SiC-supported SCALMS systems combine good catalytic performance with high durability, and 550 °C was identified as the best temperature for propane dehydrogenation with these systems. At these conditions, support-induced coking was low and Pt-based dehydrogenation activity was high. It is interesting to note that even at 500 and 550 °C, where propene selectivity was high and hardly any coke was observed, the catalysts still showed some deactivation. This could hint for other deactivation mechanisms than coking or fouling, although we cannot rule out few atom layers of coke deposition on the catalyst as this would be below the detection limit of our HRTGA-MS.

## ■ ASSOCIATED CONTENT

### Supporting Information

The Supporting Information is available free of charge at <https://pubs.acs.org/doi/10.1021/acscatal.1c01924>.

Experimental setup, N<sub>2</sub>-sorption results, relative activity vs TOS for all catalysts, cumulative productivities, post run SEM-EDX, CO<sub>2</sub> integral signal from MS for TPO measurements, Raman spectroscopy of spent catalyst, reference experiments with pure Pt and Ga on different support, particles size distribution on as-prepared and spent catalyst (PDF)

## ■ AUTHOR INFORMATION

### Corresponding Author

**Peter Wasserscheid** – Friedrich-Alexander-Universität Erlangen-Nürnberg (FAU), Lehrstuhl für Chemische Reaktionstechnik (CRT), 91058 Erlangen, Germany; Forschungszentrum Jülich GmbH, Helmholtz-Institute Erlangen-Nürnberg for Renewable Energy (IEK-11), 91058 Erlangen, Germany; [orcid.org/0000-0003-0413-9539](https://orcid.org/0000-0003-0413-9539); Email: [peter.wasserscheid@fau.de](mailto:peter.wasserscheid@fau.de)

### Authors

**Narayanan Raman** – Friedrich-Alexander-Universität Erlangen-Nürnberg (FAU), Lehrstuhl für Chemische Reaktionstechnik (CRT), 91058 Erlangen, Germany  
**Moritz Wolf** – Friedrich-Alexander-Universität Erlangen-Nürnberg (FAU), Lehrstuhl für Chemische Reaktionstechnik (CRT), 91058 Erlangen, Germany; Forschungszentrum Jülich GmbH, Helmholtz-Institute Erlangen-Nürnberg for Renewable Energy (IEK-11), 91058 Erlangen, Germany; [orcid.org/0000-0002-1326-5337](https://orcid.org/0000-0002-1326-5337)

**Martina Heller** – Friedrich-Alexander-Universität Erlangen-Nürnberg (FAU), Lehrstuhl für Werkstoffwissenschaften, 91058 Erlangen, Germany

**Nina Heene-Würl** – Friedrich-Alexander-Universität Erlangen-Nürnberg (FAU), Lehrstuhl für Chemische Reaktionstechnik (CRT), 91058 Erlangen, Germany

**Nicola Taccardi** – Friedrich-Alexander-Universität Erlangen-Nürnberg (FAU), Lehrstuhl für Chemische Reaktionstechnik (CRT), 91058 Erlangen, Germany

**Marco Haumann** – Friedrich-Alexander-Universität Erlangen-Nürnberg (FAU), Lehrstuhl für Chemische Reaktionstechnik (CRT), 91058 Erlangen, Germany; [orcid.org/0000-0002-3896-365X](https://orcid.org/0000-0002-3896-365X)

**Peter Felber** – Friedrich-Alexander-Universität Erlangen-Nürnberg (FAU), Lehrstuhl für Werkstoffwissenschaften, 91058 Erlangen, Germany

Complete contact information is available at:

<https://pubs.acs.org/doi/10.1021/acscatal.1c01924>

### Notes

The authors declare no competing financial interest.

## ■ ACKNOWLEDGMENTS

Financial support by the European Research Council is gratefully acknowledged (Project 786475: Engineering of Supported Catalytically Active Liquid Metal Solutions). Some of the authors (M.He., M.Ha., P.F., P.W.) also acknowledge support by the Deutsche Forschungsgemeinschaft (DFG, German Research Foundation) in the frame of the SFB 1452 (Project-ID 431791331). Contributions of Walter Parada to PDH catalyst testing and of Markus Brey to the coke analysis are gratefully acknowledged.

## ■ REFERENCES

- (1) Taccardi, N.; Grabau, M.; Debuschewitz, J.; Distaso, M.; Brandl, M.; Hock, R.; Maier, F.; Papp, C.; Erhard, J.; Neiss, C.; Peukert, W.; Gorling, A.; Steinruck, H. P.; Wasserscheid, P. Gallium-rich Pd-Ga phases as supported liquid metal catalysts. *Nat. Chem.* **2017**, *9*, 862–867.
- (2) Raman, N.; Maisel, S.; Grabau, M.; Taccardi, N.; Debuschewitz, J.; Wolf, M.; Wittkamper, H.; Bauer, T.; Wu, M.; Haumann, M.; Papp, C.; Gorling, A.; Spiecker, E.; Libuda, J.; Steinruck, H. P.; Wasserscheid, P. Highly Effective Propane Dehydrogenation Using Ga-Rh Supported Catalytically Active Liquid Metal Solutions. *ACS Catal.* **2019**, *9*, 9499–9507.
- (3) Bauer, T.; Maisel, S.; Blaumeiser, D.; Vecchiotti, J.; Taccardi, N.; Wasserscheid, P.; Bonivardi, A.; Gorling, A.; Libuda, J. Operando DRIFTS and DFT Study of Propane Dehydrogenation over Solid- and Liquid-Supported Ga<sub>x</sub>Pt<sub>y</sub> Catalysts. *ACS Catal.* **2019**, *9*, 2842–2853.
- (4) Sebastian, O.; Nair, S.; Taccardi, N.; Wolf, M.; Søgaard, A.; Haumann, M.; Wasserscheid, P. Stable and Selective Dehydrogenation

ation of Methylcyclohexane using Supported Catalytically Active Liquid Metal Solutions - Ga<sub>52</sub>Pt/SiO<sub>2</sub> SCALMS. *ChemCatChem* **2020**, *12*, 4533–4537.

(5) Okamoto, H.; Schlesinger, M. E.; Mueller, E. M. *Ga (Gallium) binary Alloy Phase Diagrams*; ASM International, 2016; Vol. 3.

(6) Yatsenko, S. P.; Sabirzyanov, N. A.; Yatsenko, A. S. Dissolution rates and solubility of some metals in liquid gallium and aluminum. *J. Phys.: Conf. Ser.* **2008**, *98*, 062032.

(7) Liu, J. Catalysis by Supported Single Metal Atoms. *ACS Catal.* **2017**, *7*, 34–59.

(8) Giannakakis, G.; Flytzani-Stephanopoulos, M.; Sykes, E. C. H. Single-Atom Alloys as a Reductionist Approach to the Rational Design of Heterogeneous Catalysts. *Acc. Chem. Res.* **2019**, *52*, 237–247.

(9) Furukawa, S.; Komatsu, T. Intermetallic Compounds: Promising Inorganic Materials for Well-Structured and Electronically Modified Reaction Environments for Efficient Catalysis. *ACS Catal.* **2017**, *7*, 735–765.

(10) Grabau, M.; Erhard, J.; Taccardi, N.; Calderon, S. K.; Wasserscheid, P.; Gorling, A.; Steinrueck, H. P.; Papp, C. Spectroscopic Observation and Molecular Dynamics Simulation of Ga Surface Segregation in Liquid Pd-Ga Alloys. *Chem. - Eur. J.* **2017**, *23*, 17701–17706.

(11) Rupprechter, G. Supported liquid metal catalysts: Popping up to the surface. *Nat. Chem.* **2017**, *9*, 833–834.

(12) Li, Q.; Sui, Z.; Zhou, X.; Zhu, Y.; Zhou, J.; Chen, D. Coke Formation on Pt-Sn/Al<sub>2</sub>O<sub>3</sub> Catalyst in Propane Dehydrogenation: Coke Characterization and Kinetic Study. *Top. Catal.* **2011**, *54*, 888–896.

(13) Iglesias-Juez, A.; Beale, A. M.; Maaijen, K.; Weng, T. C.; Glatzel, P.; Weckhuysen, B. M. A combined in situ time-resolved UV-Vis, Raman and high-energy resolution X-ray absorption spectroscopy study on the deactivation behavior of Pt and PtSn propane dehydrogenation catalysts under industrial reaction conditions. *J. Catal.* **2010**, *276*, 268–279.

(14) Pham, H. N.; Sattler, J. J.; Weckhuysen, B. M.; Datye, A. K. Role of Sn in the Regeneration of Pt/gamma-Al<sub>2</sub>O<sub>3</sub> Light Alkane Dehydrogenation Catalysts. *ACS Catal.* **2016**, *6*, 2257–2264.

(15) Li, C.; Minh, C. L.; Brown, T. C. Kinetics of CO and CO<sub>2</sub> Evolution During the Temperature-Programmed Oxidation of Coke Deposited on Cracking Catalysts. *J. Catal.* **1998**, *178*, 275–283.

(16) Nawaz, Z. Light alkane dehydrogenation to light olefin technologies: a comprehensive review. *Rev. Chem. Eng.* **2015**, *31*, 413–436.

(17) Li, L.; Wang, H.; Han, J.; Zhu, X.; Ge, Q. Balancing the Activity and Selectivity of Propane Oxidative Dehydrogenation on NiOOH (001) and (010). *Trans. Tianjin Univ.* **2020**, *26*, 341–351.

(18) Gambo, Y.; Adamu, S.; Abdulsheeh, A. A.; Lucky, R. A.; Ba-Shammakh, M. S.; Hossain, M. M. Catalyst design and tuning for oxidative dehydrogenation of propane - A review. *Appl. Catal., A* **2021**, *609*, 117914.

(19) Cavani, F.; Ballarini, N.; Cericola, A. Oxidative dehydrogenation of ethane and propane: How far from commercial implementation? *Catal. Today* **2007**, *127*, 113–131.

(20) Song, H.; Kim, T.; Kang, S.; Jin, H.; Lee, K.; Yoon, H. J. Ga-Based Liquid Metal Micro/Nanoparticles: Recent Advances and Applications. *Small* **2020**, *16*, No. 1903391.

(21) Daeneke, T.; Khoshmanesh, K.; Mahmood, N.; de Castro, I. A.; Esrafilzadeh, D.; Barrow, S. J.; Dickey, M. D.; Kalantar-Zadeh, K. Liquid metals: fundamentals and applications in chemistry. *Chem. Soc. Rev.* **2018**, *47*, 4073–4111.

(22) Yamaguchi, A.; Mashima, Y.; Iyoda, T. Reversible Size Control of Liquid-Metal Nanoparticles under Ultrasonication. *Angew. Chem., Int. Ed.* **2015**, *54*, 12809–12813.

(23) Kumar, V. B.; Kolytyn, Y.; Gedanken, A.; Porat, Z. E. Ultrasonic cavitation of molten gallium in water: entrapment of organic molecules in gallium microspheres. *J. Mater. Chem. A* **2014**, *2*, 1309–1317.

(24) Ghasemian, M. B.; Mayyas, M.; Idrus-Saidi, S. A.; Jamal, M. A.; Yang, J.; Mofarah, S. S.; Adabifiroozjaei, E.; Tang, J.; Syed, N.; O'Mullane, A. P.; Daeneke, T.; Kalantar-Zadeh, K. Self-Limiting Galvanic Growth of MnO<sub>2</sub> Monolayers on a Liquid Metal—Applied to Photocatalysis. *Adv. Funct. Mater.* **2019**, *29*, 1901649.

(25) Minnick, D. L.; Turnaoglu, T.; Rocha, M. A.; Shiflett, M. B. Review Article: Gas and vapor sorption measurements using electronic beam balances. *J. Vac. Sci. Technol., A* **2018**, *36*, 050801.

(26) The MathWorks Inc. *MATLAB, 2018b*; MathWorks: Natick, MA, 2018.

(27) O'Haver, T. *peakfit.m, Version 9.0, MATLAB File Exchange*; MathWorks: Natick, MA, 2018.

(28) Shriver, D. F.; Shirk, A. E. Trihydrido(trimethylamine)gallium. *Inorg. Synth.* **1980**, *17*, 42–44.

(29) Wolf, M.; Raman, N.; Taccardi, N.; Horn, R.; Haumann, M.; Wasserscheid, P. Capturing spatially resolved kinetic data and coking of Ga-Pt Supported Catalytically Active Liquid Metal Solutions during propane dehydrogenation in situ. *Faraday Discuss.* **2021**, *229*, 359–377.

(30) Wolf, M.; Raman, N.; Taccardi, N.; Haumann, M.; Wasserscheid, P. Coke Formation during Propane Dehydrogenation over Ga-Rh Supported Catalytically Active Liquid Metal Solutions. *ChemCatChem* **2020**, *12*, 1085–1094.

(31) Hohner, C.; Kettner, M.; Stumm, C.; Blaumeiser, D.; Wittkämper, H.; Grabau, M.; Schwarz, M.; Schuschke, C.; Lykhach, Y.; Papp, C.; Steinrueck, H.-P.; Libuda, J. Pt-Ga Model SCALMS on Modified HOPG: Thermal Behavior and Stability in UHV and under Near-Ambient Conditions. *J. Phys. Chem. C* **2020**, *124*, 2562–2573.